

---

# COMPREHENSIVE EVALUATION OF NO-REFERENCE IMAGE QUALITY ASSESSMENT ALGORITHMS ON KADID-10K DATABASE

---

Domonkos Varga

November 10, 2020

## ABSTRACT

The main goal of objective image quality assessment is to devise computational, mathematical models which are able to predict perceptual image quality consistently with subjective evaluations. The evaluation of objective image quality assessment algorithms is based on experiments conducted on publicly available benchmark databases. In this study, our goal is to give a comprehensive evaluation about no-reference image quality assessment algorithms, whose original source codes are available online, using the recently published KADID-10k database which is one of the largest available benchmark databases. Specifically, average PLCC, SROCC, and KROCC are reported which were measured over 100 random train-test splits. Furthermore, the database was divided into a train (appx. 80% of images) and a test set (appx. 20% of images) with respect to the reference images. So no semantic content overlap was between these two sets. Our evaluation results may be helpful to obtain a clear understanding about the status of state-of-the-art no-reference image quality assessment methods.

**Keywords** no-reference image quality assessment

## 1 Introduction

There are three main categories of objective image quality assessment (IQA) algorithms. Namely, IQA problems can be classified based on the availability of the reference, pristine images. In *full-reference image quality assessment (FR-IQA)*, the reference, pristine (distortion-free) image and the distorted image are given to estimate the perceptual quality of the distorted image. In contrast, *no-reference image quality assessment (NR-IQA)* algorithms solely rely on the distorted images. Similarly, in *reduced-reference image quality assessment (RR-IQA)* the reference image is not available, but partial information about it is known.

The evaluation of objective IQA algorithms is based on experiments carried out on publicly available image quality databases which consist of images labelled with quality scores. These databases can be divided into two categories based on the distortion types. The first one contains dozens of pristine (distortion free), reference images and the distorted images are derived from the reference images using different levels of artificial distortions and different types of artificial distortions, such as Gaussian blurring, JPEG compression, JPEG2000 compression, color diffusion, *etc.* The second one consists of authentically distorted images captured by various imaging devices, such as mobile camera. As a consequence, the images are afflicted by a highly complex mixture of multiple distortions. Table 1 summarizes the main characteristics of major publicly available image quality databases.

### 1.1 Contributions

The goal of this study to provide a comprehensive evaluation of several NR-IQA algorithms, including DIIVINE [14], BLIINDS-II [15], BRISQUE [16], NIQE [17], CurveletQA [18], SSEQ [19], GRAD-LOG-CP [20], PIQE [21], IL-NIQE [22], BMPRI [23], SPF-IQA [24], SCORER [25], ENIQA [26], and MultiGAP [27], on the recently published KADID-10k [13] database. As one can see from Table 1, KADID-10k [13] contains 81 reference images and 10,125

Table 1: Comparison of several publicly available IQA databases.

Database	Ref. images	Test images	Resolution	Distortion levels	Number of distortions
LIVE [1]	29	779	768 × 512	4-5	5
A57 [2]	3	54	512 × 512	6	3
Toyoma-MICT [3]	14	168	768 × 512	6	2
TID2008 [4]	25	1,700	512 × 384	4	17
CSIQ [5]	30	866	512 × 512	4-5	6
VCL-FER [6]	23	552	683 × 512	6	4
LIVE Multiple Distorted [7]	15	405	1280 × 720	3	2
TID2013 [8]	25	3,000	512 × 384	5	24
CID:IQ [9]	23	690	800 × 800	5	6
LIVE In the Wild [10]	-	1,169	500 × 500	-	N/A
MDID [11]	20	1,600	512 × 384	4	5
KonIQ-10k [12]	-	10,073	1024 × 768	-	N/A
KADID-10k [13]	81	10,125	512 × 384	5	25

distorted images using 25 different distortions in 5 levels. Table 2 summarizes the different distortion types found in KADID-10k [13]. Figure 1 and 2 illustrate the distortion types of KADID-10k [13]. Figure 3 depicts an illustration about the five different distortion levels.

Table 2: Distortion types found in KADID-10k [13].

Code	Distortion type
1	Gaussian blur
2	Lens blur
3	Motion blur
4	Color diffusion
5	Color shift
6	Color quantization
7	Color saturation 1.
8	Color saturation 2.
9	JPEG2000
10	JPEG
11	White noise
12	White noise in color component
13	Impulse noise
14	Multiplicative noise
15	Denoise
16	Brighten
17	Darken
18	Mean shift
19	Jitter
20	Non-eccentricity patch
21	Pixelate
22	Quantization
23	Color block
24	High sharpen
25	Contrast change

## 1.2 Structure

The rest of this study is organized as follows. After this short introduction, Section 2 gives a brief overview about NR-IQA methods with a special attention to those algorithms which are evaluated in this study on KADID-10k [13] database. Section demonstrates experimental results and analysis. Finally, a conclusion is drawn in Section 4.



(a) Gaussian blur.



(b) Lens blur.



(c) Motion blur.



(d) Color diffusion.



(e) Color shift.



(f) Color quantization.



(g) Color saturation 1.



(h) Color saturation 2.



(i) JPEG2000.



(j) JPEG.



(k) White noise.



(l) White noise color component.



(m) Impulse noise.



(n) Multiplicative noise.



(o) Denoise.

Figure 1: Distortion types of KADID-10k.



Figure 2: Distortion types of KADID-10k.

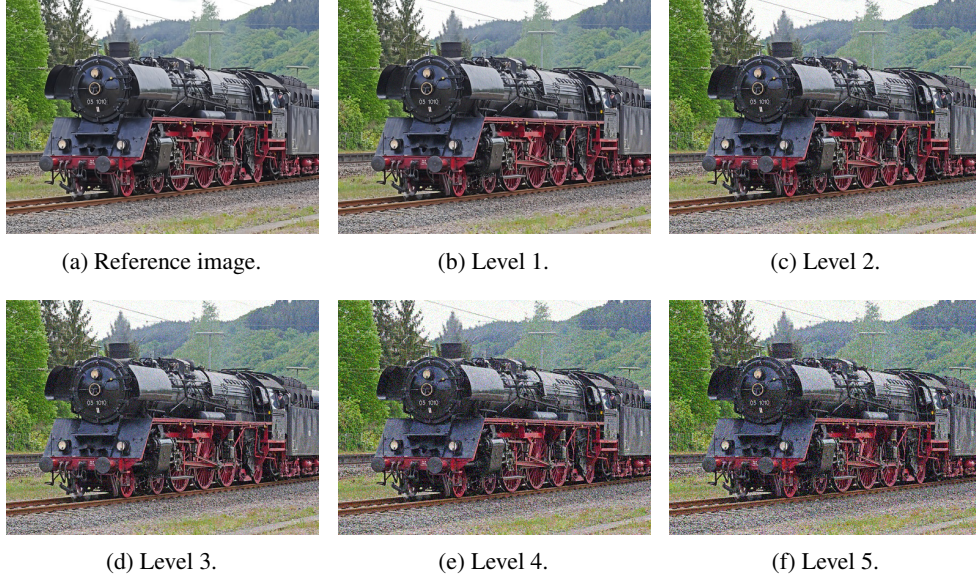


Figure 3: Illustration of distortion levels (white noise in color component).

## 2 Methods

As already mentioned, the aim of NR-IQA is to estimate the perceptual quality of a given image without any information about the pristine (distortion free), reference image. Due to the lack of any knowledge about the reference medium, NR-IQA is considered more challenging than FR-IQA or RR-IQA. Although the reference image is not available in NR-IQA, assumptions can be made about the distortion types found in an image, such as JPEG2000 compression noise. *Distortion-specific* methods assume one specific distortion type in the image, while *general-purpose* algorithms work over various types of distortions. Furthermore, general-purpose can be divided into natural scene statistics (NSS) based, learning based, and human visual system (HVS) based groups. Another classification of NR-IQA methods divides existing methods into *opinion-aware* and *opinion-unaware* classes. Opinion-aware methods utilize subject scores during the training process, while opinion-unaware methods derive features from the pristine, reference images of the database and perceptual quality of distorted images is quantified as the deviation from the pristine images' features. In the followings, the examined methods are briefly discussed.

**DIIVINE** [14] is a two-stage framework which involves distortion identification and distortion-specific quality assessment. It is based on NSS. Namely, a set of neighboring wavelet coefficients were modelled by a Gaussian scale mixture model. Moreover, steerable pyramid decomposition was used to extract statistics from the distorted images.

**BLINDS-II** [15] derives NSS features by discrete cosine transform coefficients modeling using generalized Gaussian distribution. The parameters of the generalized Gaussian distribution were applied as quality-aware features.

**BRISQUE** [16] applies scene statistics of locally normalized luminance coefficients to train a support vector regressor (SVR) for perceptual quality prediction.

**NIQE** [17] measures the distance between the natural scene statistics (NSS) based features calculated from the pristine images to the features extracted from the input image. The features are modeled as multi-dimensional Gaussian distributions.

**CurveletQA** [18] extracted statistical features (the coordinates of the maxima of the log-histograms of the curvelet coefficients, the energy distributions of both orientation and scale in the curvelet domain) from the image's curvelet representation. Moreover, image distortion and quality prediction stages are trained using a support vector machine (SVM).

**SSEQ** [19] contains an image distortion and quality prediction engine. Furthermore, it extracts a 12-dimensional local entropy feature vector.

**GRAD-LOG-CP** [20] utilizes the joint statistics of gradient magnitude map and the Laplacian of Gaussian features to train a support vector regressor (SVR) for perceptual image quality prediction.

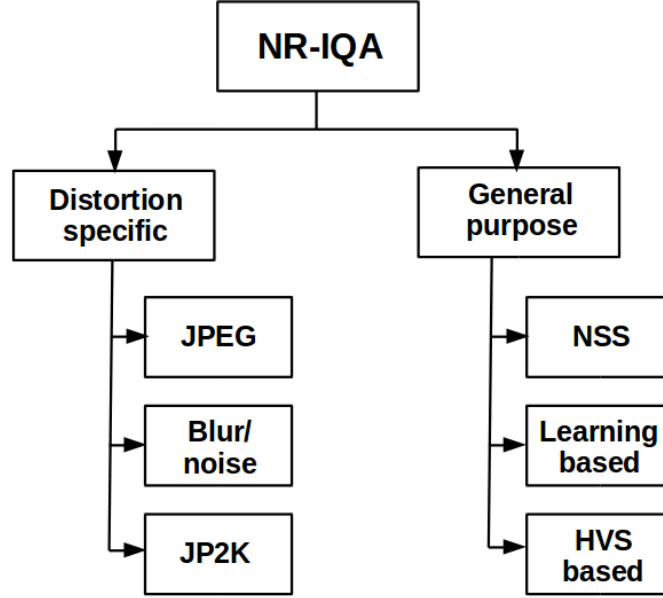


Figure 4: Classification of no-reference image quality assessment.

**PIQE** [21] is an opinion-unaware method and calculates perceptual quality of an image through block-wise distortion estimation. First, the mean subtracted contrast normalized (MSCN) coefficients are determined for each pixel in the input image. Second, the input image is divided into  $16 \times 16$  blocks and high spatially active blocks are identified relying on the MSCN coefficients. In each block, distortion is evaluated due to blocking artifacts and noise relying on the MSCN coefficients. A threshold criteria is also applied to classify blocks as distorted (blocking artifacts, Gaussian noise) blocks. The quality score is computed as the mean of scores in the distorted blocks.

**IL-NIQE** [22] is an opinion-unaware method. It integrated natural image statistics features from multiple sources, such as normalized luminance, mean subtracted and contrast normalized coefficients, gradient statistics, statistics of log-Gabor filter responses, and statistics of colors. Subsequently, a multivariate Gaussian model is learned from pristine image patches. Perceptual quality is quantified by measuring the deviation from the learned distribution using a Bhattacharyya-like distance.

**BMPRI** [23] introduced the concept of multiple pseudo reference images (MPRI). Specifically, the distorted images were further degraded. Subsequently, similarities between the distorted image and the MPRI were measured. To this end, a traditional FR-IQA metric was applied. Specifically, local binary pattern features were computed to describe the similarities between the distorted image and the MPRI. Finally, the similarity scores were aggregated to obtain the input image's perceptual quality.

**SPF-IQA** [24] extracted different statistical (fractal dimension distribution, first digit distribution in gradient magnitude domain, first digit distribution in wavelet domain, color statistics) and perceptual features (colorfulness, global contrast factor, dark channel feature, entropy, mean of phase congruency) from the input image and fused them together. Finally, the fused feature vector is mapped onto perceptual quality scores with the help of Gaussian process regression (GPR) using rational quadratic kernel function.

**SCORER** [25] proposed a set of derivative kernels which were utilized to filter the  $Y$ ,  $Cb$ , and  $Cr$  channels of the input image. As a result, a set of filtered images was obtained for further processing. Subsequently,  $N$  interest points were detected on each filtered image relying on features from accelerated segment test (FAST) [28]. Specifically, each interest point is used to describe a  $3 \times 3$  block around the interest point by taking all values from the block. The extracted 2400-dimensional feature vectors are mapped onto perceptual quality scores with the help of a trained support vector regressor (SVR).

**ENIQA** [26] extracts features in two different domains. Namely, mutual information between color channels and the two-dimensional entropy is determined first. Subsequently, two-dimensional entropy and the mutual information of the filtered sub-band images are determined. Based on the extracted features, a support vector machine (SVM) and a support vector regressor (SVR) is trained for distortion and quality prediction, respectively.

In **MultiGAP** [27], an input image is run through an Inception-V3 pretrained convolutional neural network which carries out all its defined operations. Moreover, global average pooling layers are attached to each Inception module to extract image resolution independent features. Subsequently, the features of the Inception modules are concatenated and mapped onto perceptual quality scores with the help of an support vector regressor (SVR) with Gaussian kernel function. In this study, results obtained by Gaussain process regression (GPR) head with rational quadratic function is also presented.

### 3 Experimental results and analysis

In this section, we report on the experimental results obtained on KADID-10k [13] database. The rest of this section is organized as follows. In Subsection 3.1, the evaluation metrics are defined. Subsection 3.2 describes the experimental setup. In Subsection 3.3, the performance of the examined NR-IQA algorithms is reported on the entire KADID-10k [13]. Subsection 3.4 reports the performance on individual distortion levels, while Subsection 3.5 presents the experimental results with respect to the distortion types.

#### 3.1 Evaluation metrics

As already mentioned, the evaluation of IQA algorithms is based on the correlation between the predicted and ground-truth scores measured on an image quality database. In the literature, there are three major evaluation: Pearson’s linear correlation coefficient (PLCC), Spearman’s rank order correlation coefficient (SROCC), and Kendall’s rank order correlation coefficient (KROCC). The latter two measure the prediction monotonicity of an IQA method, because they operate merely on the rank of the data points and ignore the relative distance between data points. MATLAB provides functions for the computation of these performance metrics.

```

1 PLCC = corr(groundScores, predictedScores);
2 SROCC= corr(groundScores, predictedScores, 'Type', 'Spearman');
3 KROCC= corr(groundScores, predictedScores, 'Type', 'Kendall');

```

The PLCC between two data sets,  $A$  and  $B$ , is defined as

$$PLCC(A, B) = \frac{\sum_{i=1}^n (A_i - \bar{A})(B_i - \bar{B})}{\sqrt{\sum_{i=1}^n (A_i - \bar{A})^2} \sqrt{\sum_{i=1}^n (B_i - \bar{B})^2}}, \quad (1)$$

where  $\bar{A} = \frac{1}{n} \sum_{i=1}^n A_i$  and  $\bar{B} = \frac{1}{n} \sum_{i=1}^n B_i$ . SROCC between  $A$  and  $B$  datasets is defined as

$$SROCC(A, B) = PLCC(rank(A), rank(B)), \quad (2)$$

where the  $rank(\cdot)$  function gives back a vector whose  $i$ th element is the rank of the  $i$ th element in the input vector. KROCC is defined as

$$KROCC(A, B) = \frac{n_c - n_d}{\frac{1}{2}n(n-1)}, \quad (3)$$

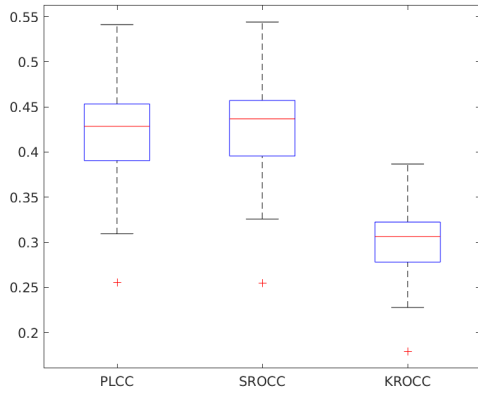
where  $n$  is the length of  $A$  and  $B$ ,  $n_c$  denotes the number of concordant pairs between  $A$  and  $B$ , and  $n_d$  is the number of discordant pairs.

#### 3.2 Experimental setup

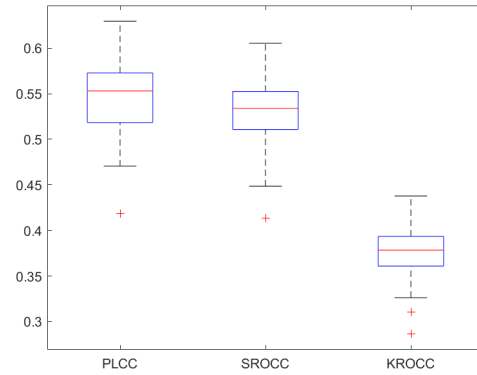
For learning-based methods, the distorted images of KADID-10k [13] were divided into a training (appx. 80% of images) and a test set (appx. 20% of images) with respect to the reference images. As a consequence, there was no semantic overlap between these two sets. Moreover, average PLCC, SROCC, and KROCC were measured over 100 random train-test splits. In contrast, opinion-unaware methods were trained on the reference images and tested on the distorted images. Furthermore, PLCC, SROCC, and KROCC are reported.

#### 3.3 Overall performance

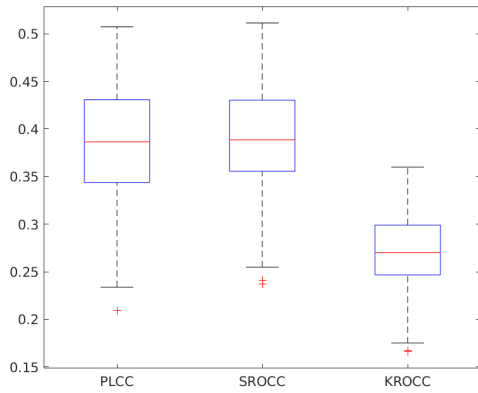
The performance of the examined algorithms in terms of average PLCC, SROCC, and KROCC (100 random train-test splits) is summarized in Table 3. From these results, it can be observed that SCORER [25] performs significantly better than any other NR-IQA algorithms. MultiGAP-GPR [27] took the second, MultiGAP-SVR [27] took the third, and SPF-IQA [24] took the fourth place, respectively. The boxplot figures of the 100 random train-test splits are depicted in Figures 5 and 6. On each box, the central mark indicates the median, and the bottom and top edges of the box indicate the 25th and 75th percentiles, respectively. The whiskers extend to the most extreme data points not considered outliers. Moreover, the outliers are plotted by ‘+’.



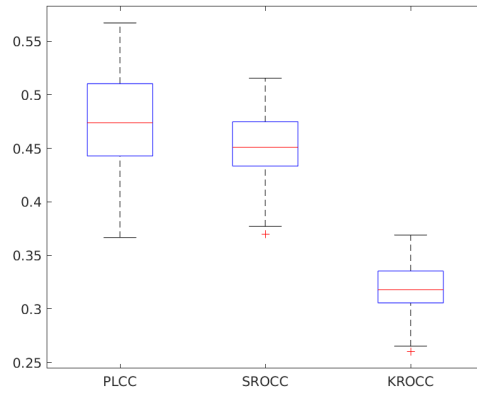
(a) DIIVINE.



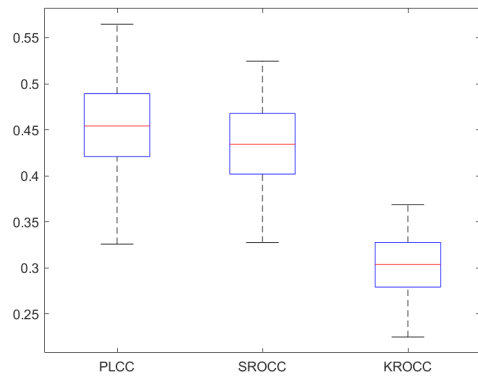
(b) BLIINDS-II.



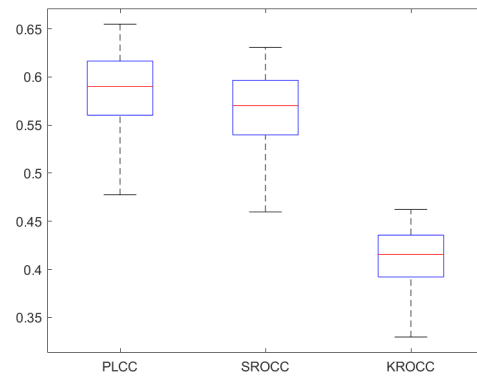
(c) BRISQUE.



(d) CurveletQA.



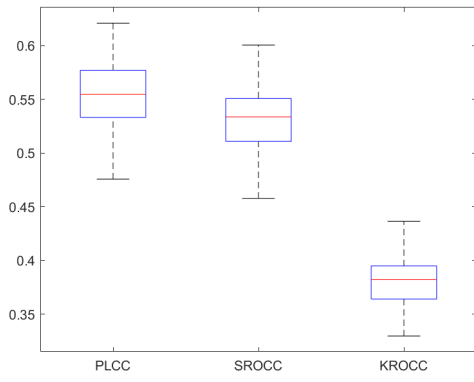
(e) SSEQ.



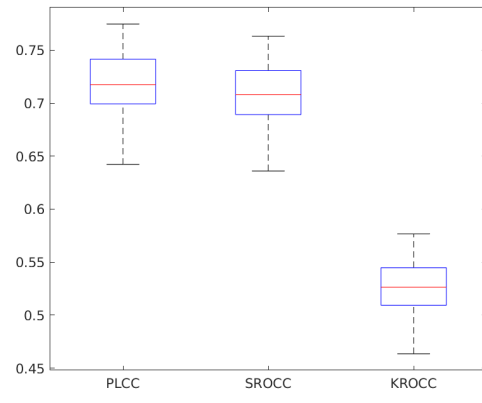
(f) GRAD-LOG-CP.

Figure 5: Box plots of the measured PLCC, SROCC, and KROCC values. 100 random train-test splits.

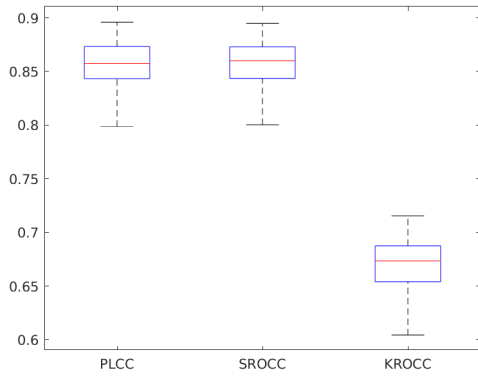




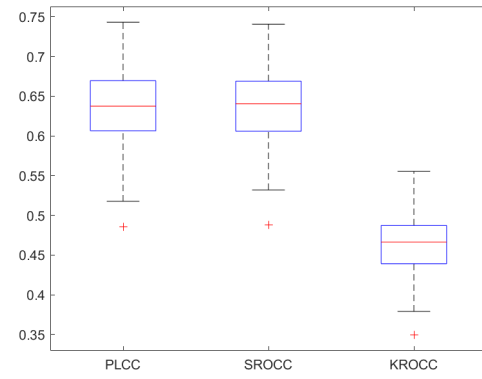
(a) BMPRI.



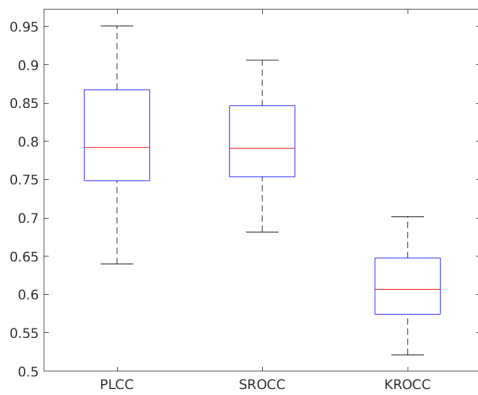
(b) SPF-IQA.



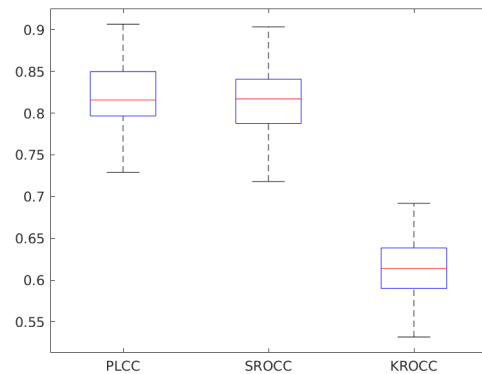
(c) SCORER.



(d) ENIQA.



(e) MultiGAP-SVR.



(f) MultiGAP-GPR.

Figure 6: Box plots of the measured PLCC, SROCC, and KROCC values. 100 random train-test splits.

Table 3: Overall performance on KADID-10k [13]. Average PLCC, SROCC, and KROCC are reported, measured 100 random train-test splits. The best results are typed by **bold**, the second best results are typed by *italic*.

Method	PLCC	SROCC	KROCC
DIIVINE [14]	0.423	0.428	0.302
BLIINDS-II [15]	0.548	0.530	0.377
BRISQUE [16]	0.383	0.386	0.269
NIQE [17]	0.273	0.309	0.309
CurveletQA [18]	0.473	0.450	0.318
SSEQ [19]	0.453	0.433	0.302
GRAD-LOG-CP [20]	0.585	0.566	0.411
PIQE [21]	0.289	0.237	0.237
IL-NIQE [22]	0.230	0.211	0.211
BMPRI [23]	0.554	0.530	0.379
SPF-IQA [24]	0.717	0.708	0.526
SCORER [25]	<b>0.855</b>	<b>0.856</b>	<b>0.669</b>
ENIQA [26]	0.634	0.636	0.464
MultiGAP-SVR [27]	0.799	0.795	0.608
MultiGAP-GPR [27]	<i>0.820</i>	<i>0.814</i>	<i>0.613</i>

### 3.4 Performance over different distortion levels

In this subsection, the performance of the examined NR-IQA algorithms is given over different distortion levels. Specifically, Tables 4, 5, and 6 summarize the average PLCC, SROCC, and KROCC values over the different distortion levels of KADID-10k database [13].

Table 4: Performance over different distortion levels of KADID-10k [13]. Average PLCC is reported, measured over 100 random train-test splits.

	Level1	Level2	Level3	Level4	Level5
DIIVINE [14]	0.026	0.158	0.281	0.365	0.455
BLIINDS-II [15]	0.163	0.239	0.376	0.503	0.558
BRISQUE [16]	0.071	0.148	0.198	0.339	0.441
NIQE [17]	0.036	0.061	0.045	0.101	0.137
CurveletQA [18]	0.088	0.185	0.317	0.412	0.495
SSEQ [19]	0.055	0.143	0.265	0.360	0.498
GRAD-LOG-CP [20]	0.126	0.300	0.412	0.495	0.562
PIQE [21]	0.032	-0.007	0.048	0.115	0.248
IL-NIQE [22]	0.003	0.084	0.127	0.153	0.120
BMPRI [23]	0.097	0.265	0.399	0.478	0.545
SPF-IQA [24]	0.241	0.465	0.606	0.694	0.721
SCORER [25]	0.490	0.742	0.806	0.844	0.787
ENIQA [26]	0.165	0.382	0.504	0.595	0.644
MultiGAP-SVR [27]	0.336	0.472	0.631	0.725	0.782
MultiGAP-GPR [27]	0.424	0.577	0.730	0.825	0.889

### 3.5 Performance over different distortion types

In this subsection, the performance of the examined NR-IQA algorithms is given over different distortion types. Specifically, Tables 7, 8, and 9 summarize the average PLCC, SROCC, and KROCC values over the different distortion types of KADID-10k database [13]. As already mentioned, Table 2 summarizes the different distortions types found in KADID-10k [13] and their numeric codes.

Table 5: Performance over different distortion levels of KADID-10k [13]. Average SROCC is reported, measured over 100 random train-test splits.

	Level1	Level2	Level3	Level4	Level5
DIIVINE [14]	-0.007	0.152	0.285	0.411	0.528
BLIINDS-II [15]	0.172	0.228	0.358	0.535	0.629
BRISQUE [16]	0.064	0.150	0.199	0.360	0.473
NIQE [17]	0.141	0.126	0.065	0.104	0.162
CurveletQA [18]	0.082	0.186	0.309	0.417	0.532
SSEQ [19]	0.007	0.127	0.246	0.363	0.548
GRAD-LOG-CP [20]	0.103	0.298	0.403	0.513	0.605
PIQE [21]	0.052	-0.005	0.007	0.061	0.207
IL-NIQE [22]	0.024	0.095	0.126	0.129	0.100
BMPRI [23]	0.096	0.256	0.386	0.495	0.588
SPF-IQA [24]	0.212	0.458	0.603	0.691	0.741
SCORER [25]	0.436	0.737	0.818	0.839	0.769
ENIQA [26]	0.127	0.373	0.505	0.610	0.688
MultiGAP-SVR [27]	0.331	0.475	0.662	0.781	0.842
MultiGAP-GPR [27]	0.407	0.563	0.728	0.839	0.906

Table 6: Performance over different distortion levels of KADID-10k [13]. Average KROCC is reported, measured over 100 random train-test splits.

	Level1	Level2	Level3	Level4	Level5
DIIVINE [14]	0.026	0.158	0.281	0.365	0.455
BLIINDS-II [15]	0.163	0.239	0.376	0.503	0.558
BRISQUE [16]	0.071	0.148	0.198	0.339	0.441
NIQE [17]	0.036	0.061	0.045	0.101	0.137
CurveletQA [18]	0.088	0.185	0.317	0.412	0.495
SSEQ [19]	0.055	0.143	0.265	0.360	0.498
GRAD-LOG-CP [20]	0.126	0.300	0.412	0.495	0.562
PIQE [21]	0.032	-0.007	0.048	0.115	0.248
IL-NIQE [22]	0.003	0.084	0.127	0.153	0.120
BMPRI [23]	0.097	0.265	0.399	0.478	0.545
SPF-IQA [24]	0.241	0.465	0.606	0.694	0.721
SCORER [25]	0.490	0.742	0.806	0.844	0.787
ENIQA [26]	0.165	0.382	0.504	0.595	0.644
MultiGAP-SVR [27]	0.282	0.382	0.516	0.605	0.651
MultiGAP-GPR [27]	0.332	0.442	0.565	0.653	0.709

## 4 Conclusion

In this study, several NR-IQA algorithms, including DIIVINE [14], BLIINDS-II [15], BRISQUE [16], NIQE [17], CurveletQA [18], SSEQ [19], GRAD-LOG-CP [20], PIQE [21], IL-NIQE [22], BMPRI [23], SPF-IQA [24], SCORER [25], ENIQA [26], MultiGAP-SVR [27], and MultiGAP-GPR [27], were evaluated on KADID-10k [13] database.

## References

- [1] Hamid R Sheikh, Muhammad F Sabir, and Alan C Bovik. A statistical evaluation of recent full reference image quality assessment algorithms. *IEEE Transactions on image processing*, 15(11):3440–3451, 2006.
- [2] Damon M Chandler and Sheila S Hemami. Vsnr: A wavelet-based visual signal-to-noise ratio for natural images. *IEEE transactions on image processing*, 16(9):2284–2298, 2007.
- [3] Yuukou Horita, Keiji Shibata, Yoshikazu Kawayoke, and ZM Parvez Sazzad. Mict image quality evaluation database. *Online*, <http://mict.eng.u-toyama.ac.jp/mictdb.html>, 2011.

- [4] Nikolay Ponomarenko, Vladimir Lukin, Alexander Zelensky, Karen Egiazarian, Marco Carli, and Federica Battisti. Tid2008-a database for evaluation of full-reference visual quality assessment metrics. *Advances of Modern Radioelectronics*, 10(4):30–45, 2009.
- [5] Eric Cooper Larson and Damon Michael Chandler. Most apparent distortion: full-reference image quality assessment and the role of strategy. *Journal of electronic imaging*, 19(1):011006, 2010.
- [6] Anđela Zarić, Nenad Tatalović, Nikolina Brajković, Hrvoje Hlevnjak, Matej Lončarić, Emil Dumić, and Sonja Grgić. Vcl@fer image quality assessment database. *AUTOMATIKA: časopis za automatiku, mjerenje, elektroniku, računarstvo i komunikacije*, 53(4):344–354, 2012.
- [7] Dinesh Jayaraman, Anish Mittal, Anush K Moorthy, and Alan C Bovik. Objective quality assessment of multiply distorted images. In *2012 Conference record of the forty sixth asilomar conference on signals, systems and computers (ASILOMAR)*, pages 1693–1697. IEEE, 2012.
- [8] Nikolay Ponomarenko, Lina Jin, Oleg Ieremeiev, Vladimir Lukin, Karen Egiazarian, Jaakko Astola, Benoit Vozel, Kacem Chehdi, Marco Carli, Federica Battisti, et al. Image database tid2013: Peculiarities, results and perspectives. *Signal Processing: Image Communication*, 30:57–77, 2015.
- [9] Xinwei Liu, Marius Pedersen, and Jon Yngve Hardeberg. Cid: Iq—a new image quality database. In *International Conference on Image and Signal Processing*, pages 193–202. Springer, 2014.
- [10] Deepti Ghadiyaram and Alan C Bovik. Massive online crowdsourced study of subjective and objective picture quality. *IEEE Transactions on Image Processing*, 25(1):372–387, 2015.
- [11] Wen Sun, Fei Zhou, and Qingmin Liao. Mdid: A multiply distorted image database for image quality assessment. *Pattern Recognition*, 61:153–168, 2017.
- [12] Hanhe Lin, Vlad Hosu, and Dietmar Saupe. Koniq-10k: Towards an ecologically valid and large-scale iqa database. *arXiv preprint arXiv:1803.08489*, 2018.
- [13] Hanhe Lin, Vlad Hosu, and Dietmar Saupe. Kadid-10k: A large-scale artificially distorted iqa database. In *2019 Eleventh International Conference on Quality of Multimedia Experience (QoMEX)*, pages 1–3. IEEE, 2019.
- [14] Anush Krishna Moorthy and Alan Conrad Bovik. Blind image quality assessment: From natural scene statistics to perceptual quality. *IEEE transactions on Image Processing*, 20(12):3350–3364, 2011.
- [15] Michele A Saad, Alan C Bovik, and Christophe Charrier. Blind image quality assessment: A natural scene statistics approach in the dct domain. *IEEE transactions on Image Processing*, 21(8):3339–3352, 2012.
- [16] Anish Mittal, Anush Krishna Moorthy, and Alan Conrad Bovik. No-reference image quality assessment in the spatial domain. *IEEE Transactions on image processing*, 21(12):4695–4708, 2012.
- [17] Anish Mittal, Rajiv Soundararajan, and Alan C Bovik. Making a “completely blind” image quality analyzer. *IEEE Signal processing letters*, 20(3):209–212, 2012.
- [18] Lixiong Liu, Hongping Dong, Hua Huang, and Alan C Bovik. No-reference image quality assessment in curvelet domain. *Signal Processing: Image Communication*, 29(4):494–505, 2014.
- [19] Lixiong Liu, Bao Liu, Hua Huang, and Alan Conrad Bovik. No-reference image quality assessment based on spatial and spectral entropies. *Signal Processing: Image Communication*, 29(8):856–863, 2014.
- [20] Wufeng Xue, Xuanqin Mou, Lei Zhang, Alan C Bovik, and Xiangchu Feng. Blind image quality assessment using joint statistics of gradient magnitude and laplacian features. *IEEE Transactions on Image Processing*, 23(11):4850–4862, 2014.
- [21] N Venkatanath, D Praneeth, Maruthi Chandrasekhar Bh, Sumohana S Channappayya, and Swarup S Medasani. Blind image quality evaluation using perception based features. In *2015 Twenty First National Conference on Communications (NCC)*, pages 1–6. IEEE, 2015.
- [22] Lin Zhang, Lei Zhang, and Alan C Bovik. A feature-enriched completely blind image quality evaluator. *IEEE Transactions on Image Processing*, 24(8):2579–2591, 2015.
- [23] Xiongkuo Min, Guangtao Zhai, Ke Gu, Yutao Liu, and Xiaokang Yang. Blind image quality estimation via distortion aggravation. *IEEE Transactions on Broadcasting*, 64(2):508–517, 2018.
- [24] Domonkos Varga. No-reference image quality assessment based on the fusion of statistical and perceptual features. *Journal of Imaging*, 6(8):75, 2020.
- [25] Mariusz Oszust. Local feature descriptor and derivative filters for blind image quality assessment. *IEEE Signal Processing Letters*, 26(2):322–326, 2019.

- [26] Xiaoqiao Chen, Qingyi Zhang, Manhui Lin, Guangyi Yang, and Chu He. No-reference color image quality assessment: from entropy to perceptual quality. *EURASIP Journal on Image and Video Processing*, 2019(1):77, 2019.
- [27] Domonkos Varga. Multi-pooled inception features for no-reference image quality assessment. *Applied Sciences*, 10(6):2186, 2020.
- [28] Edward Rosten and Tom Drummond. Machine learning for high-speed corner detection. In *European conference on computer vision*, pages 430–443. Springer, 2006.

Table 7: Performance over different distortion types of KADID-10k [13]. Average PLCC is reported, measured over 100 random train-test splits.

	1	2	3	4	5	6	7	8	9	10	11	12	13	14	15	16	17	18	19	20	21	22	23	24	25
DIVINE [14]	0.691	0.818	0.581	0.249	0.300	0.433	-0.020	0.086	0.558	0.672	0.454	0.541	0.459	0.480	0.777	0.204	0.221	0.037	0.612	0.065	0.432	0.383	0.041	0.608	0.105
BLINDS-II [15]	0.799	0.772	0.412	0.602	0.016	0.499	0.094	0.530	0.690	0.806	0.529	0.684	0.583	0.563	0.685	0.438	0.556	0.232	0.843	0.045	0.651	0.315	0.166	0.583	0.116
BRISQUE [16]	0.764	0.808	0.461	0.192	0.180	0.403	0.091	0.240	0.057	0.598	0.350	0.437	0.411	0.428	0.642	0.433	0.258	0.093	0.679	0.135	0.416	0.378	0.098	0.507	0.039
NIQE [17]	0.760	0.291	0.628	0.242	-0.123	0.585	-0.044	0.244	0.647	0.930	0.641	0.746	0.791	0.655	0.807	0.516	0.538	0.242	0.869	0.102	0.466	0.759	0.056	0.440	0.180
CurveletQA [18]	0.821	0.851	0.714	0.228	0.109	0.653	0.020	0.081	0.665	0.634	0.691	0.719	0.591	0.612	0.777	0.426	0.524	0.078	0.634	0.078	0.142	0.339	0.037	0.589	0.027
SSQE [19]	0.716	0.723	0.368	0.366	0.031	0.556	0.075	0.210	0.560	0.800	0.622	0.664	0.556	0.581	0.570	0.315	0.395	0.115	0.571	0.026	0.523	0.218	0.165	0.566	0.086
GRAD-LOG-GP [20]	0.826	0.842	0.526	0.363	0.021	0.735	-0.028	0.320	0.764	0.887	0.816	0.844	0.685	0.723	0.845	0.470	0.463	0.168	0.839	0.072	0.778	0.598	0.302	0.674	0.138
PIQE [21]	0.902	0.773	0.311	0.264	-0.052	0.700	0.067	0.164	0.813	0.820	0.774	0.865	0.601	0.815	-0.234	0.468	0.501	0.117	-0.293	0.047	0.403	0.696	-0.016	0.376	-0.059
IL-NIQE [22]	0.475	0.488	0.277	-0.092	0.087	0.160	0.115	0.028	0.230	0.382	0.508	0.666	0.518	0.477	0.676	-0.128	-0.200	-0.035	0.378	-0.014	0.324	-0.295	0.015	0.243	0.045
BMPRI [23]	0.844	0.810	0.393	0.386	0.117	0.704	0.094	0.431	0.723	0.927	0.807	0.729	0.424	0.565	0.832	0.478	0.487	0.241	0.718	-0.016	0.677	0.334	0.141	0.495	0.130
SPE-IQA [24]	0.845	0.829	0.546	0.800	0.289	0.761	0.124	0.761	0.685	0.865	0.880	0.901	0.699	0.750	0.884	0.686	0.502	0.143	0.726	0.080	0.791	0.704	0.354	0.809	0.236
SCORER [25]	0.925	0.929	0.846	0.813	0.722	0.776	0.030	0.820	0.896	0.929	0.897	0.928	0.894	0.902	0.927	0.773	0.784	0.267	0.913	0.318	0.787	0.798	0.483	0.806	0.362
ENIQA [26]	0.778	0.792	0.576	0.819	0.226	0.651	0.035	0.687	0.709	0.847	0.748	0.769	0.608	0.708	0.782	0.570	0.470	0.159	0.668	0.011	0.546	0.537	0.102	0.677	0.178
MultiGAP-SVR [27]	0.842	0.830	0.715	0.874	0.631	0.416	0.390	0.765	0.751	0.898	0.572	0.616	0.611	0.660	0.830	0.677	0.493	0.219	0.790	0.329	0.693	0.502	0.530	0.709	0.153
MultiGAP-GPR [27]	0.966	0.940	0.857	0.979	0.755	0.664	0.446	0.848	0.916	0.932	0.710	0.756	0.769	0.804	0.932	0.799	0.623	0.295	0.937	0.426	0.793	0.674	0.584	0.834	0.232

Table 8: Performance over different distortion types of KADID-10k [13]. Average SROCC is reported, measured over 100 random train-test splits.

	1	2	3	4	5	6	7	8	9	10	11	12	13	14	15	16	17	18	19	20	21	22	23	24	25
DIIVINE [14]	0.719	0.803	0.584	0.324	0.217	0.399	-0.008	0.089	0.515	0.624	0.473	0.543	0.453	0.504	0.801	0.176	0.166	0.026	0.597	0.067	0.394	0.386	0.051	0.636	0.072
BLINDS-II [15]	0.791	0.761	0.405	0.529	0.029	0.475	0.099	0.504	0.639	0.763	0.550	0.688	0.612	0.580	0.699	0.405	0.422	0.212	0.818	0.032	0.576	0.313	0.161	0.616	0.112
BRISQUE [16]	0.781	0.791	0.449	0.255	0.142	0.397	0.087	0.251	0.051	0.556	0.396	0.457	0.382	0.482	0.692	0.424	0.196	0.105	0.665	0.116	0.376	0.363	0.107	0.418	0.048
NIQE [17]	0.743	0.255	0.652	0.313	-0.175	0.614	-0.041	0.235	0.704	0.850	0.648	0.755	0.854	0.698	0.870	0.445	0.411	0.179	0.871	0.111	0.667	0.769	0.050	0.731	0.148
CurveletQA [18]	0.810	0.853	0.717	0.285	0.138	0.631	0.026	0.068	0.594	0.609	0.716	0.749	0.621	0.637	0.779	0.412	0.209	0.068	0.590	0.048	0.130	0.342	0.086	0.627	0.008
SSSEQ [19]	0.716	0.731	0.368	0.436	0.026	0.538	0.063	0.206	0.462	0.695	0.641	0.678	0.597	0.606	0.607	0.259	0.303	0.102	0.554	0.004	0.482	0.206	0.174	0.593	0.061
GRAD-LOG-CP [20]	0.812	0.811	0.512	0.385	0.067	0.682	-0.002	0.323	0.677	0.788	0.847	0.863	0.704	0.741	0.826	0.437	0.372	0.143	0.796	0.083	0.687	0.590	0.305	0.698	0.132
PIQE [21]	0.863	0.770	0.299	0.317	-0.008	0.727	0.064	0.159	0.758	0.768	0.811	0.875	0.582	0.828	-0.099	0.421	0.325	0.112	-0.271	0.009	0.353	0.717	-0.010	0.406	-0.028
IL-NIQE [22]	0.519	0.596	0.275	-0.097	0.018	0.162	0.113	0.009	0.189	0.335	0.528	0.680	0.576	0.488	0.719	-0.134	-0.166	-0.028	0.363	-0.032	0.297	-0.303	0.035	0.247	0.026
BMPRI [23]	0.843	0.817	0.594	0.453	0.106	0.669	0.118	0.444	0.618	0.820	0.837	0.753	0.461	0.598	0.823	0.438	0.374	0.197	0.699	0.004	0.540	0.296	0.146	0.520	0.133
SPE-IQA [24]	0.835	0.802	0.537	0.791	0.306	0.722	0.110	0.770	0.601	0.802	0.889	0.914	0.714	0.773	0.883	0.644	0.382	0.140	0.709	0.096	0.715	0.703	0.369	0.821	0.225
SCORER [25]	0.898	0.885	0.841	0.751	0.661	0.761	0.053	0.811	0.844	0.812	0.902	0.923	0.892	0.911	0.916	0.732	0.658	0.230	0.874	0.332	0.701	0.778	0.408	0.810	0.388
ENIQA [26]	0.785	0.795	0.572	0.673	0.162	0.629	0.050	0.671	0.636	0.773	0.766	0.790	0.611	0.732	0.814	0.528	0.354	0.100	0.651	0.006	0.482	0.527	0.119	0.702	0.170
MultiGAP-SVR [27]	0.915	0.895	0.775	0.898	0.665	0.406	0.387	0.832	0.746	0.902	0.623	0.670	0.660	0.714	0.916	0.681	0.437	0.266	0.842	0.358	0.696	0.520	0.568	0.810	0.173
MultiGAP-GPR [27]	0.975	0.964	0.873	0.983	0.758	0.634	0.433	0.872	0.837	0.980	0.721	0.771	0.791	0.823	0.965	0.747	0.523	0.310	0.928	0.432	0.736	0.644	0.600	0.893	0.238

Table 9: Performance over different distortion types of KADID-10k [13]. Average KROCC is reported, measured over 100 random train-test splits.

	1	2	3	4	5	6	7	8	9	10	11	12	13	14	15	16	17	18	19	20	21	22	23	24	25
DIVINE [14]	0.691	0.818	0.581	0.249	0.300	0.433	-0.020	0.086	0.558	0.672	0.454	0.541	0.459	0.480	0.777	0.204	0.221	0.037	0.612	0.065	0.432	0.383	0.041	0.608	0.105
BLINDS-II [15]	0.799	0.772	0.412	0.602	0.016	0.499	0.094	0.530	0.690	0.806	0.529	0.684	0.583	0.563	0.685	0.438	0.556	0.232	0.843	0.045	0.651	0.315	0.166	0.583	0.116
BRSQUE [16]	0.764	0.808	0.461	0.192	0.180	0.403	0.091	0.240	0.057	0.598	0.350	0.437	0.411	0.428	0.642	0.433	0.258	0.093	0.679	0.135	0.416	0.378	0.098	0.507	0.039
NIQE [17]	0.760	0.291	0.628	0.242	-0.123	0.585	-0.044	0.244	0.647	0.930	0.641	0.746	0.791	0.655	0.807	0.516	0.538	0.242	0.869	0.102	0.466	0.759	0.056	0.440	0.180
CurveletQA [18]	0.821	0.851	0.714	0.228	0.109	0.653	0.020	0.081	0.665	0.634	0.691	0.719	0.591	0.612	0.777	0.426	0.524	0.078	0.634	0.078	0.142	0.339	0.037	0.589	0.027
SSSEQ [19]	0.716	0.723	0.368	0.366	0.031	0.556	0.075	0.210	0.560	0.800	0.622	0.664	0.556	0.581	0.570	0.315	0.395	0.115	0.571	0.026	0.523	0.218	0.165	0.566	0.086
GRAD-LOG-CP [20]	0.826	0.842	0.526	0.363	0.021	0.735	-0.028	0.320	0.764	0.887	0.816	0.844	0.685	0.723	0.845	0.470	0.463	0.168	0.839	0.072	0.778	0.598	0.302	0.674	0.138
PIQE [21]	0.902	0.773	0.311	0.264	-0.052	0.700	0.067	0.164	0.813	0.820	0.774	0.865	0.601	0.815	-0.234	0.468	0.501	0.117	-0.293	0.047	0.403	0.696	-0.016	0.376	-0.059
IL-NIQE [22]	0.475	0.488	0.277	-0.092	0.087	0.160	0.115	0.028	0.230	0.382	0.508	0.666	0.518	0.477	0.676	-0.128	-0.200	-0.035	0.378	-0.014	0.324	-0.295	0.015	0.243	0.045
BMPRI [23]	0.844	0.810	0.393	0.386	0.117	0.704	0.094	0.431	0.723	0.927	0.807	0.729	0.424	0.565	0.832	0.478	0.487	0.241	0.718	-0.016	0.677	0.334	0.141	0.495	0.130
SPE-IQA [24]	0.845	0.829	0.546	0.800	0.289	0.761	0.124	0.761	0.685	0.865	0.880	0.901	0.699	0.750	0.884	0.686	0.502	0.143	0.726	0.080	0.791	0.704	0.354	0.809	0.236
SCORER [25]	0.925	0.929	0.846	0.813	0.722	0.776	0.030	0.820	0.896	0.929	0.897	0.928	0.894	0.902	0.927	0.773	0.784	0.267	0.913	0.318	0.787	0.798	0.483	0.806	0.362
ENIQA [26]	0.778	0.792	0.576	0.719	0.226	0.651	0.035	0.687	0.709	0.847	0.748	0.769	0.608	0.708	0.782	0.570	0.470	0.159	0.668	0.011	0.546	0.537	0.102	0.677	0.178
MultiGAP-SVR [27]	0.716	0.704	0.600	0.702	0.523	0.334	0.318	0.642	0.582	0.711	0.489	0.524	0.518	0.560	0.722	0.534	0.354	0.233	0.651	0.298	0.547	0.418	0.441	0.632	0.173
MultiGAP-GPR [27]	0.778	0.765	0.685	0.796	0.598	0.501	0.353	0.684	0.664	0.793	0.572	0.605	0.622	0.649	0.773	0.589	0.418	0.268	0.730	0.355	0.580	0.516	0.469	0.710	0.220